Figure S1

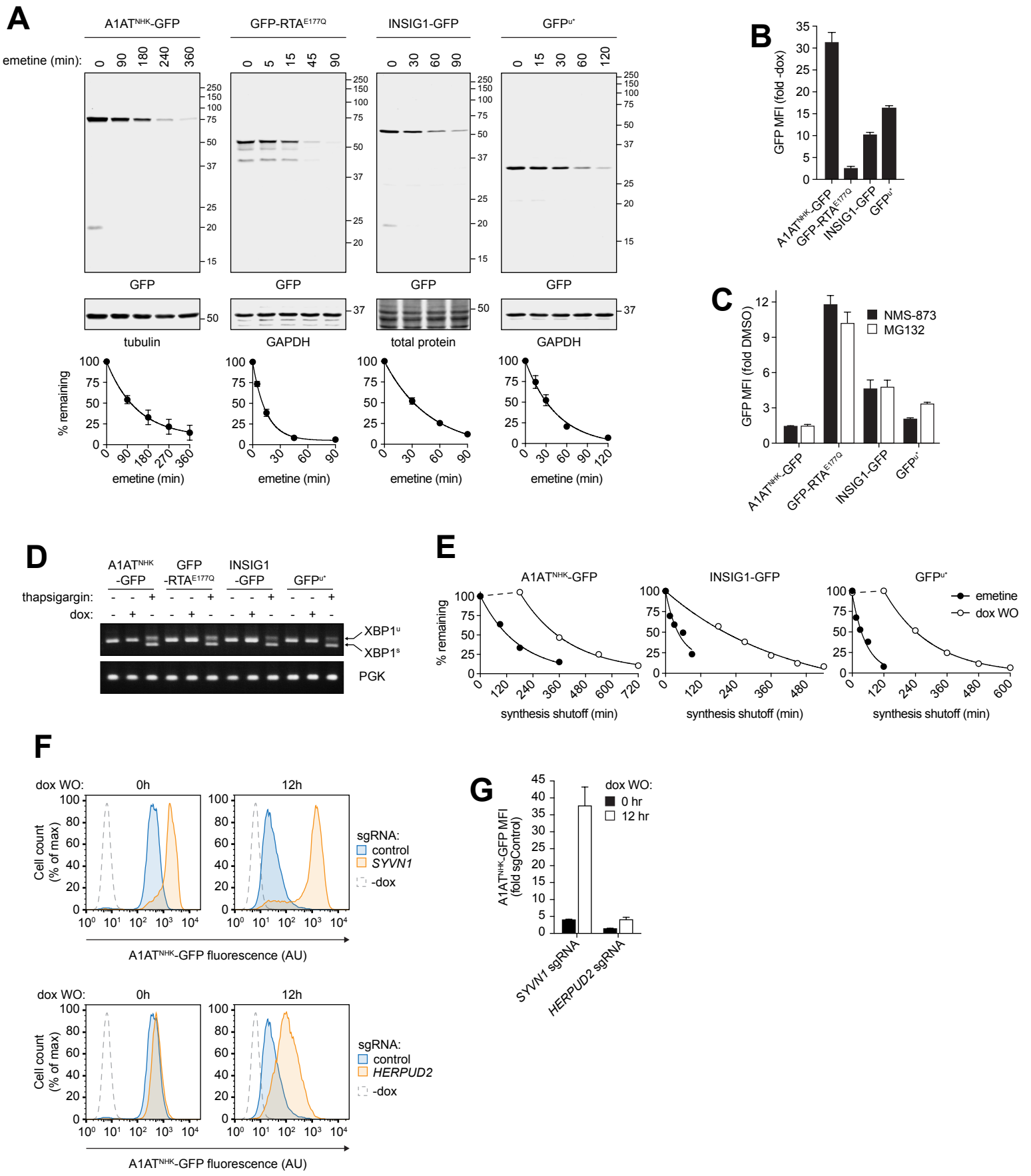

Figure S1. Related to Figure 1.Characterization of ERAD reporter cell lines. (A) Top: Immunoblots of GFP-tagged ERAD substrates treated with emetine for the indicated times to shut off protein synthesis. Bottom: Quantification of reporter turnover; data are the mean of three independent experiments ± SEM. **(B)** Fold-increase in GFP median fluorescence intensity (MFI) of reporter cells treated with dox for 16 hr; data are the mean of three independent experiments ± SEM. **(C)** Effect of 3 hr UPS inhibitor treatment on steady-state reporter fluorescence; data are the mean of three independent experiments ± SEM. **(D)** Reverse transcription PCR analysis of XBP1 splicing in the indicated cell lines treated with dox for 16 hr or thapsigargin for 1 hr. **(E)** Reporter decay after shutting off reporter transcription by removing dox (dox WO) or halting reporter translation with emetine. GFP MFI was measured at the indicated times by flow cytometry analysis; data are representative of two independent experiments. **(F)** A1AT^{NHK}-GFP K562 reporter cells expressing the indicated sgRNAs were subjected to dox washout and GFP fluorescence was measured at the indicated times by flow cytometry analysis. **(G)** Quantification of **(F)**; data are the mean of three independent experiments ± SEM.

Figure S2

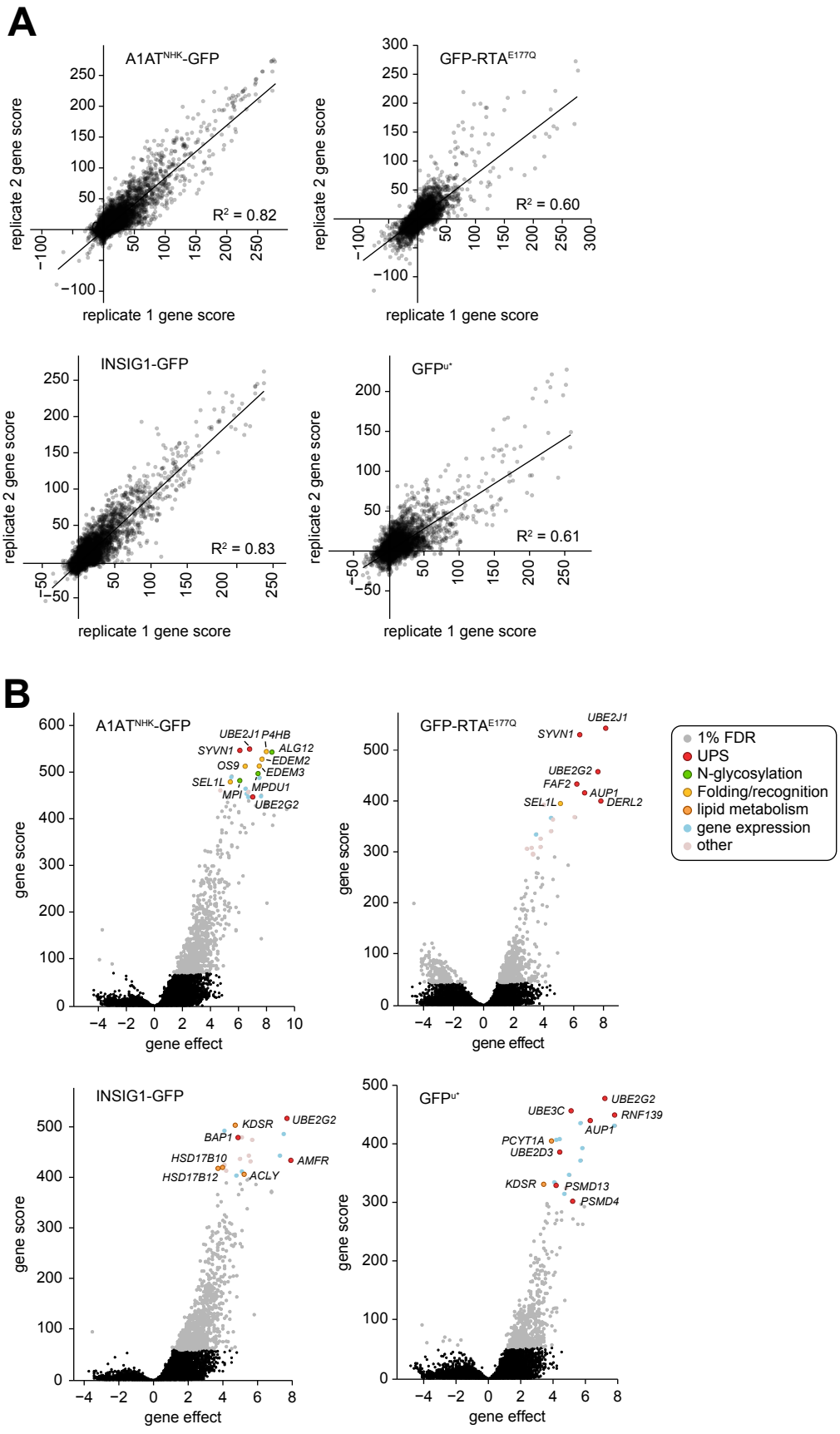

Figure S2. Related to Figure 1. ERAD screens are highly reproducible and identify essential genes. (A) Reproducibility of the genetic screens. Each reporter screen was performed twice and signed gene scores from each replicate were compared. Gene score signs were assigned based on guide enrichment, with a negative sign indicating guide disenrichment in the GFP^{high} population relative to the GFP^{low} population and a positive sign indicating guide enrichment in the GFP^{high} population relative to the GFP^{low} population. **(B)** For each screen, gene effects are plotted against gene scores. Screen hits, identified by applying a 1% false discovery rate (FDR) cutoff, are indicated in grey. The top 20 highest confidence hits from each screen are highlighted.

Figure S3

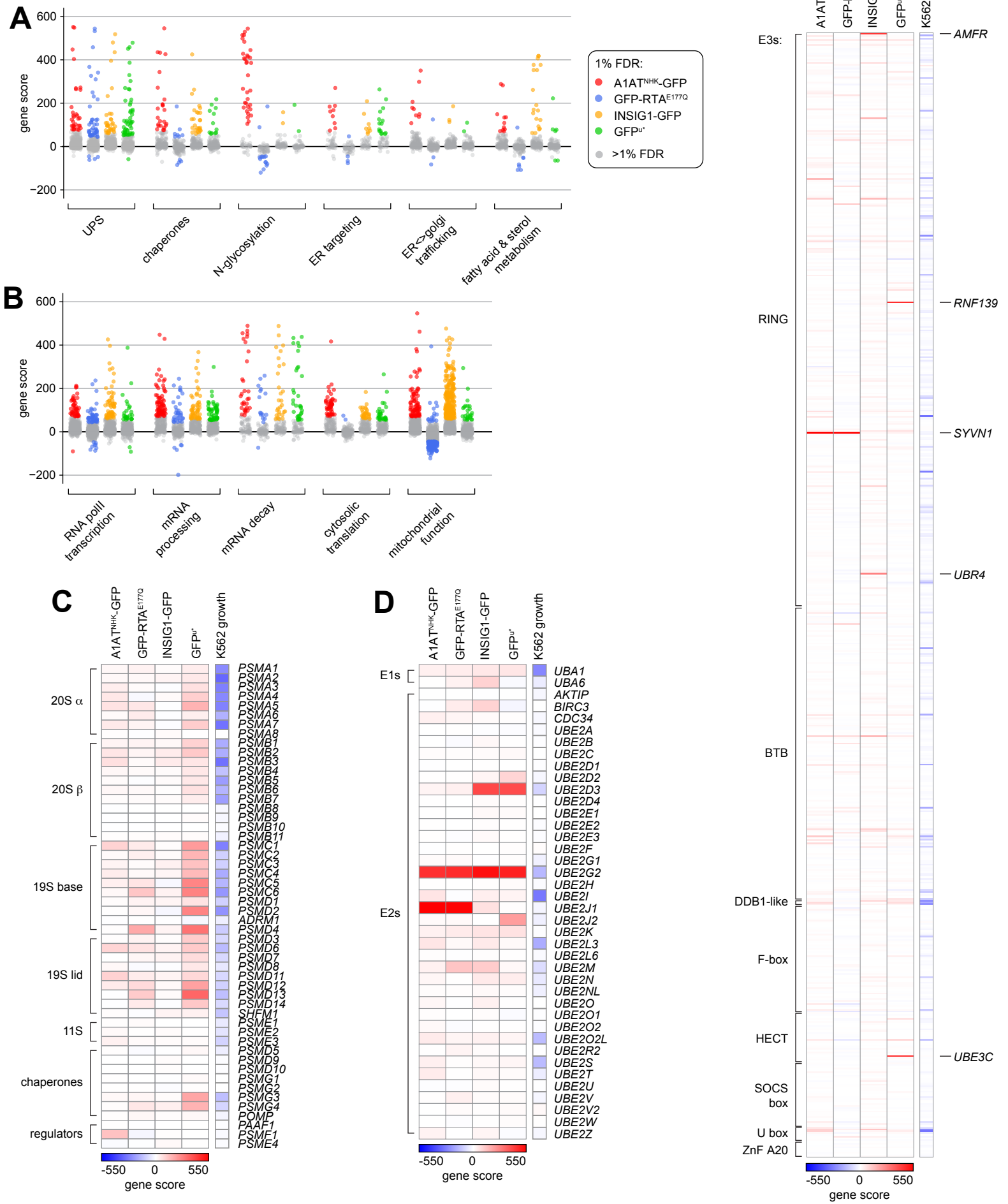

Figure S3. Related to Figure 1. Genome-wide CRISPR analysis identifies genes affecting ERAD reporter stability. (A-B) Signed gene scores for each reporter by functional category. Colored points indicate genes identified at ≤1% FDR and grey points indicate genes at >1% FDR. (A) Includes categories related to ER function and protein quality control; (B) includes categories of genes that likely exert ERAD-independent effects. **(C-E)** Heat maps of signed genes scores from the ERAD genetic screens and a K562 viability screen for all genes encoding (C) proteasome subunits, chaperones, and regulators, (D) Ub E1 and E2 enzymes, and (E) E3 Ub ligases. K562 growth data are from ref (Morgens et al., 2017). Gene score signs were assigned based on guide enrichment, with a negative sign indicating guide disenrichment in the GFP^{high} population relative to the GFP^{low} population and a positive sign indicating guide enrichment in the GFP^{high} population relative to the GFP^{low} population.

Figure S4

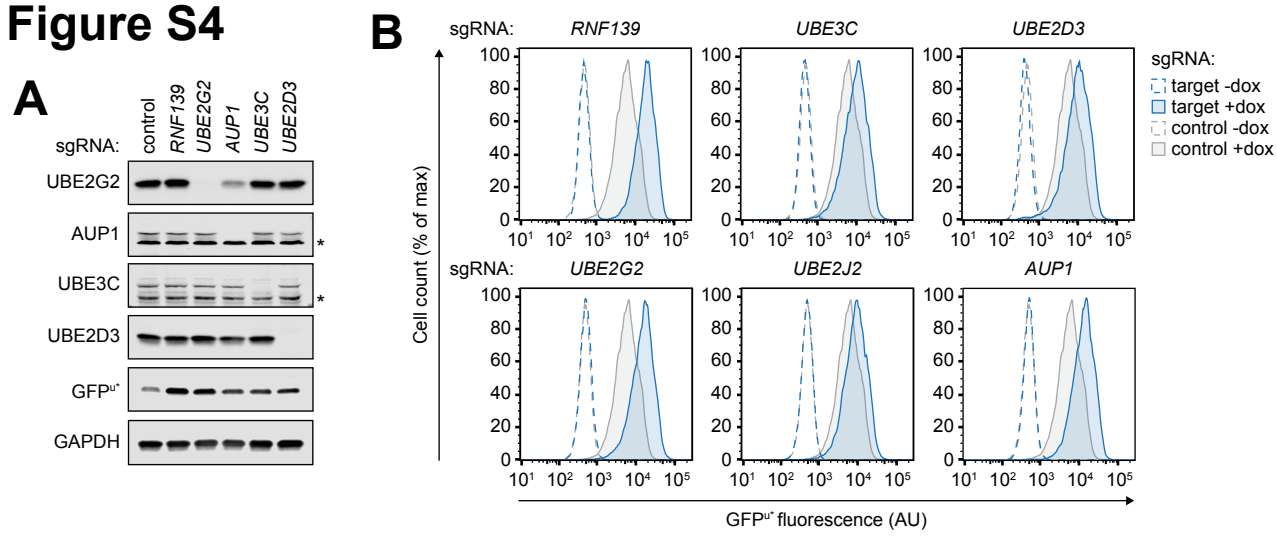

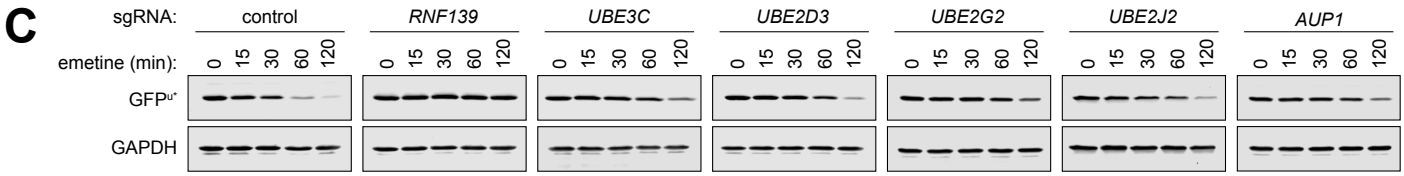

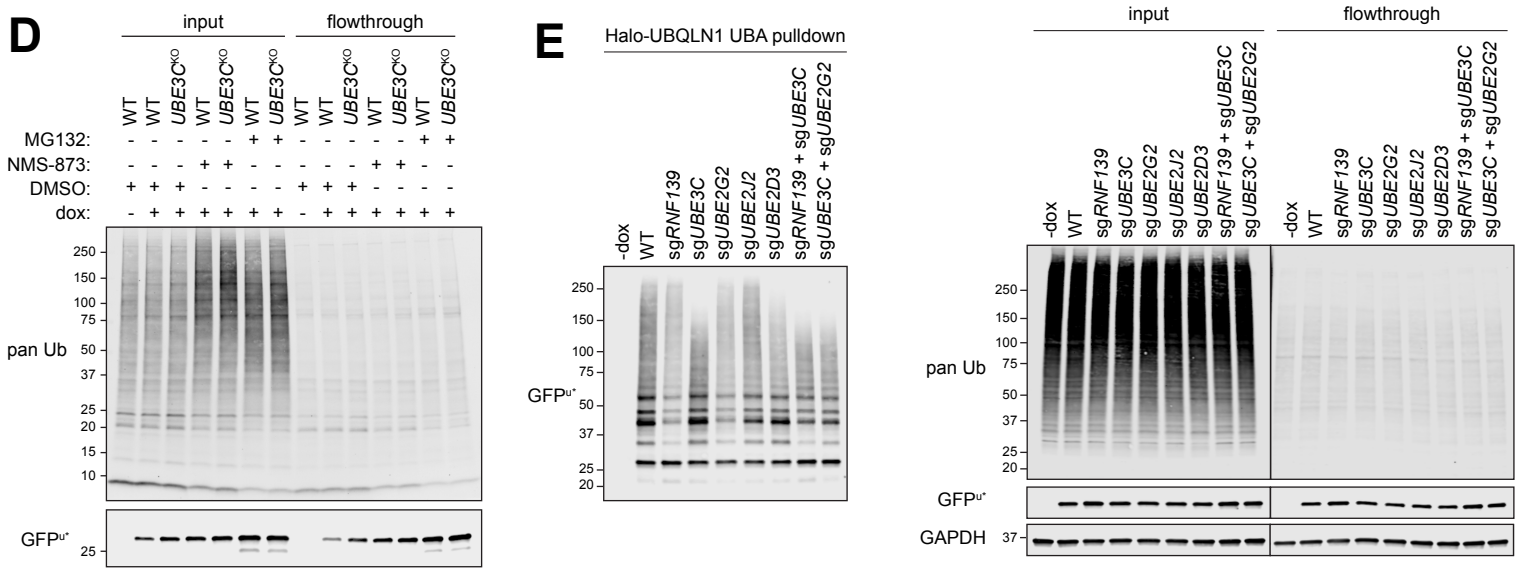

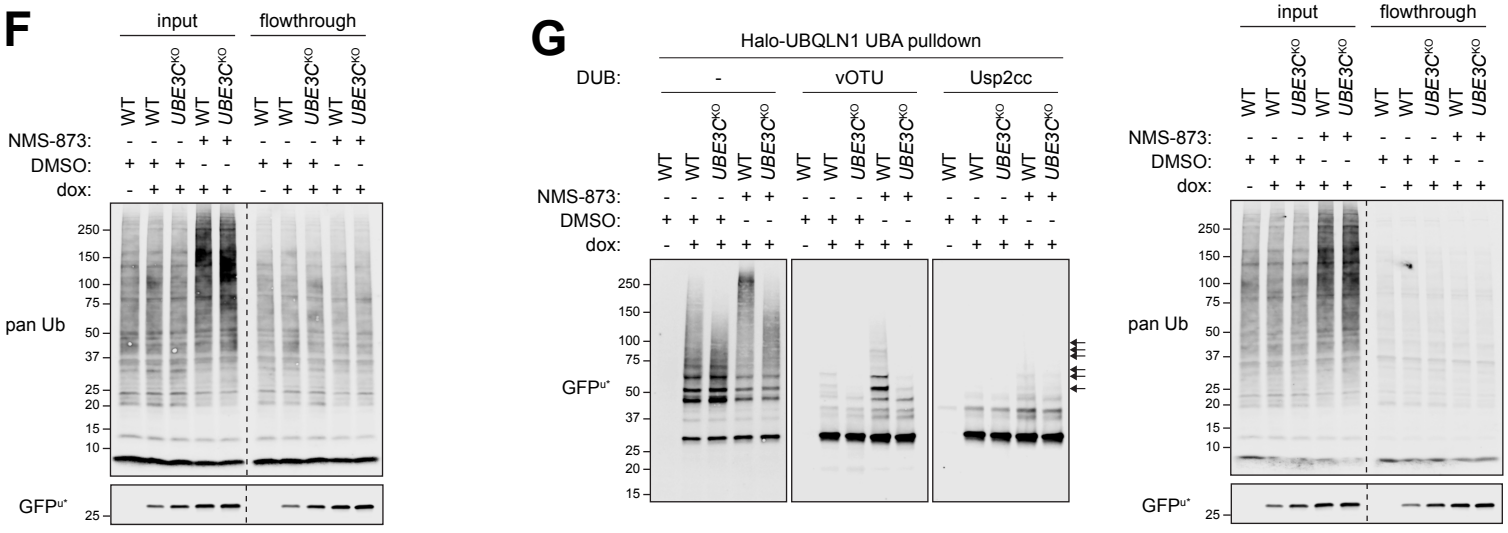

Figure S4. Related to Figure 2. Effect of ER-localized and cytosolic Ub conjugation machinery on GFP^{u*} degradation and ubiquitylation. (A) Immunoblots of lysates from GFP^{u*} reporter cells expressing the indicated sgRNAs. Asterisks indicate nonspecific bands. **(B)** Steady-state levels of dox-induced GFP^{u*} in cells expressing the indicated sgRNAs. GFP fluorescence was determined by flow cytometry analysis. **(C)** Immunoblot analysis of dox-induced GFP^{u*} reporter cells expressing the indicated individual sgRNAs and treated with emetine for the indicated times; representative of three independent experiments. See Fig. 2A for quantification. **(D)** Immunoblot analysis of cell lysate inputs and Halo-UBQLN1 UBA flowthroughs from Fig. 2F. **(E)** PolyUb conjugates were affinity captured from lysates from cells expressing the indicated sgRNA using immobilized Halo-UBQLN1 UBA. Left: Immunoblot of affinity captured Ub_n-GFP^{u*}. Right: Input and flowthrough samples were immunoblotted on separate membranes. **(F)** Immunoblot analysis of cell lysate inputs and Halo-TRABID NZF1 flowthroughs from Fig. 2I. Samples were immunoblotted on the same membrane and are displayed with the same exposure time; dashed line indicates removal of irrelevant gel lanes. **(G)** PolyUb conjugates affinity captured from cell lysates using immobilized Halo-UBQLN1 UBA were treated with the indicated DUBs for 1 hr. Left: Immunoblot of affinity captured Ub_n-GFP^{u*}. Right: Input and flowthrough samples were immunoblotted on the same membrane and are displayed with the same exposure time; dashed line indicates removal of irrelevant lanes.

Figure S5

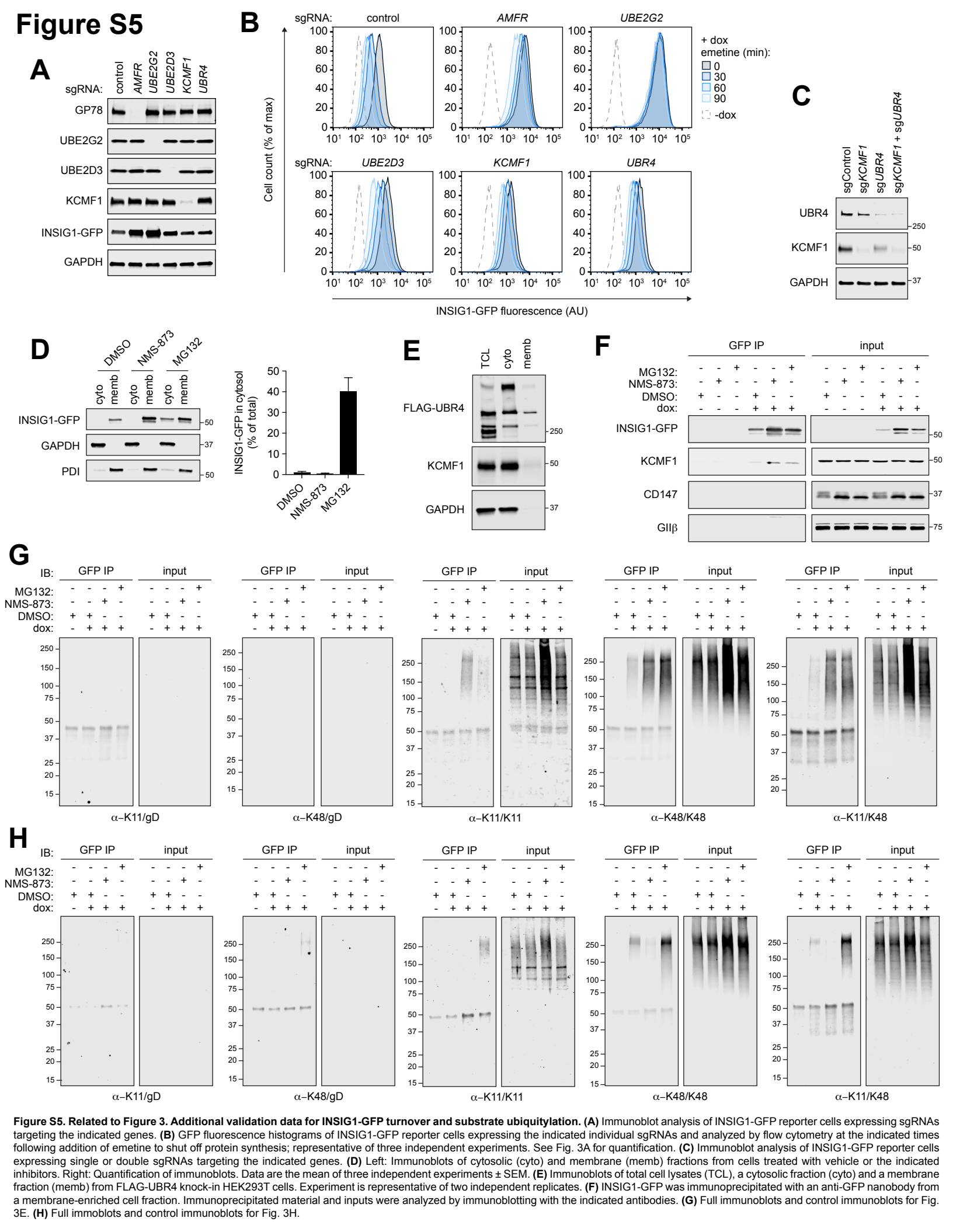

Figure S5. Related to Figure 3. Additional validation data for INSIG1-GFP turnover and substrate ubiquitylation. (A) Immunoblot analysis of INSIG1-GFP reporter cells expressing sgRNAs targeting the indicated genes. **(B)** GFP fluorescence histograms of INSIG1-GFP reporter cells expressing the indicated individual sgRNAs and analyzed by flow cytometry at the indicated times following addition of emetine to shut off protein synthesis; representative of three independent experiments. See Fig. 3A for quantification. **(C)** Immunoblot analysis of INSIG1-GFP reporter cells expressing single or double sgRNAs targeting the indicated genes. **(D)** Left: Immunoblots of cytosolic (cyto) and membrane (memb) fractions from cells treated with vehicle or the indicated inhibitors. Right: Quantification of immunoblots. Data are the mean of three independent experiments ± SEM. **(E)** Immunoblots of total cell lysates (TCL), a cytosolic fraction (cyto) and a membrane fraction (memb) from FLAG-UBR4 knock-in HEK293T cells. Experiment is representative of two independent replicates. **(F)** INSIG1-GFP was immunoprecipitated with an anti-GFP nanobody from a membrane-enriched cell fraction. Immunoprecipitated material and inputs were analyzed by immunoblotting with the indicated antibodies. **(G)** Full immunoblots and control immunoblots for Fig. 3E. **(H)** Full immoblots and control immunoblots for Fig. 3H.

Figure S6

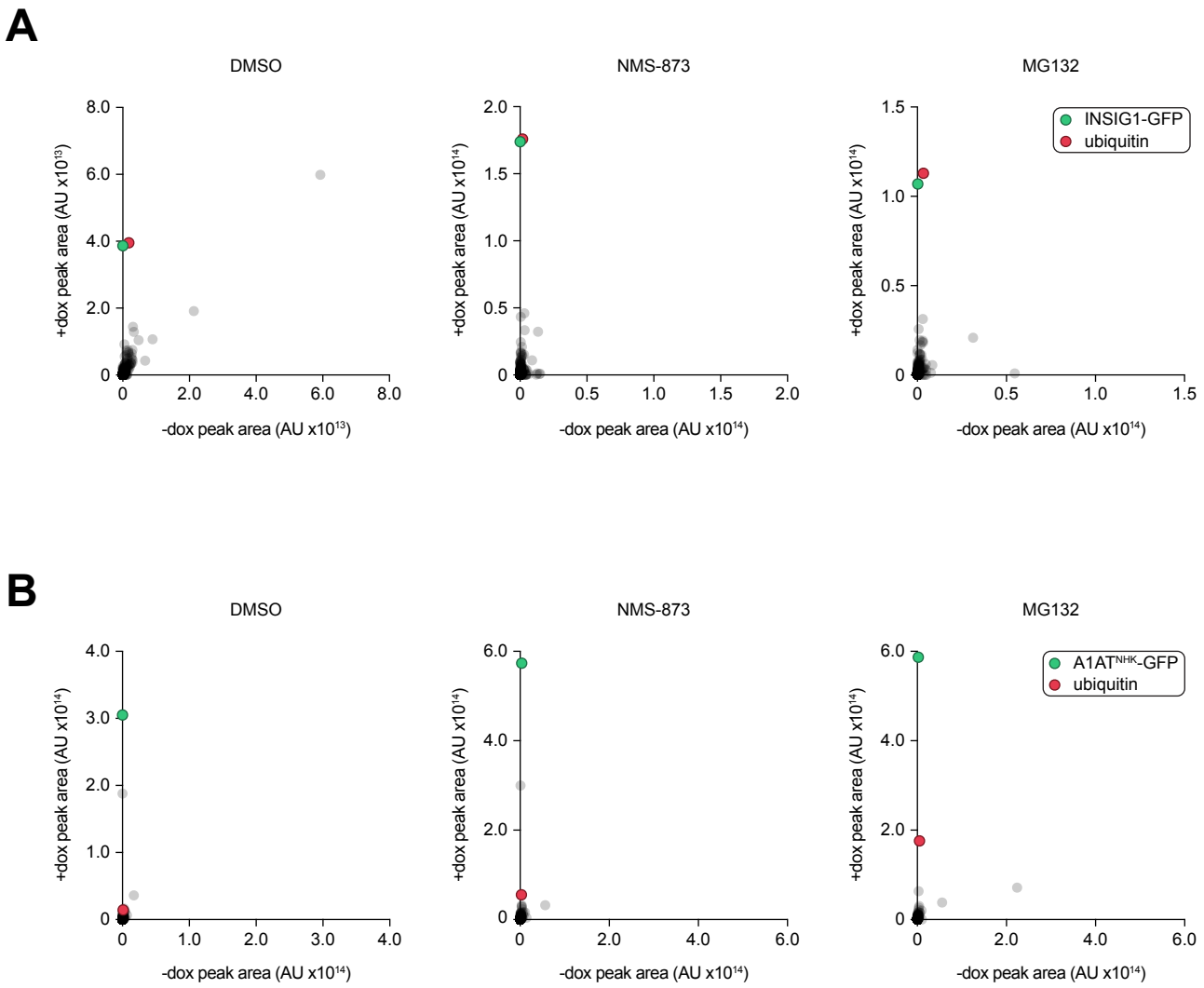

Figure S6. Related to Figure 3. Proteins identified by LC-MS/MS analysis. (A-B) Plots of proteins identified in GFP immunoisolates from urea-denatured lysates treated ± dox and with the indicated inhibitors. Peak area was calculated as the average integrated MS ion peak intensity of the top 3 unique peptides for each protein. (A) INSIG1-GFP immunoisolates; (B) A1AT^{NHK}-GFP immunoisolates.

Figure S7

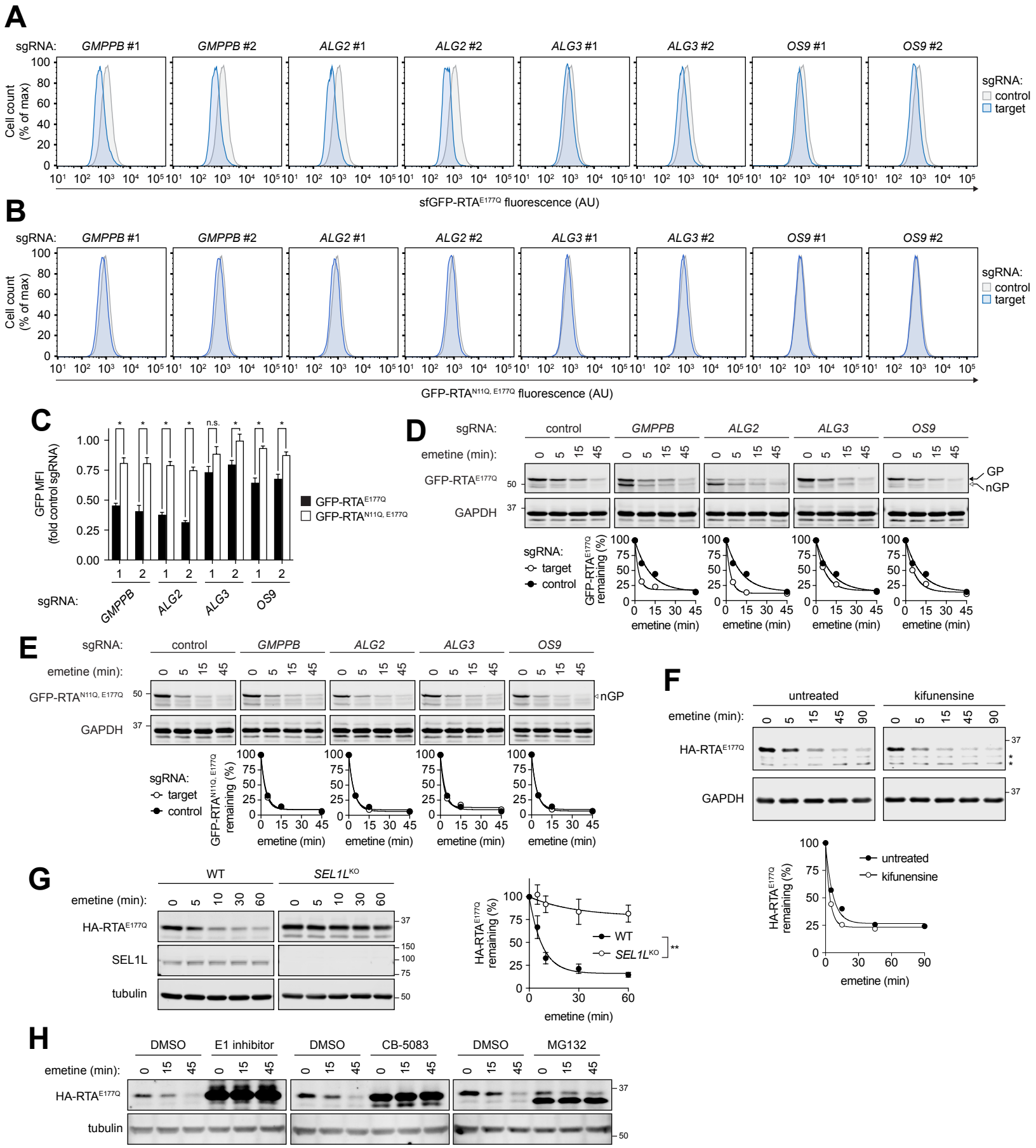

Figure S7. Related to Figure 4. GFP-RTA^{E177Q} degradation is accelerated by deletion of N-glycan biosynthesis and quality control machinery. (A-B) Flow cytometry histograms of steady-state GFP fluorescence in dox-induced reporter cells expressing (A) GFP-RTA^{E177Q} or (B) GFP-RTA$^{N11Q, E177Q}$ and the indicated sgRNAs; representative of three independent experiments. **(C)** Quantification of GFP-RTA^{E177Q} and GFP-RTA$^{N11Q, E177Q}$ levels measured by flow cytometry analysis in cells expressing the indicated sgRNAs; bars are the mean of three independent experiments ± SEM. *P ≤ 0.02 determined by Student's t-test. **(D-E)** Top: Immunoblots of (D) GFP-RTA^{E177Q} or (E) GFP-RTA$^{N11Q, E177Q}$ turnover in cells expressing the indicated sgRNAs and treated with emetine for the indicated times. Glycosylated (GP) and nonglycosylated (nGP) GFP-RTA^{E177Q} are indicated by filled and open arrows, respectively. Bottom: Quantification of reporter turnover; representative of two independent replicates. **(F)** Top: Immunoblots of HA-RTA^{E177Q} turnover in HEK293 cells treated with kifunensine for 6 hr and emetine for the indicated times. Asterisks indicate nonspecific bands. Bottom: Quantification of immunoblots. Data are representative of two independent experiments. **(G)** Left: Immunoblots of HA-RTA^{E177Q} turnover in wild-type or *SEL1L*^{KO} HEK293 cells treated with emetine for the indicated times. Right: Quantification of reporter turnover; data are the mean of three independent experiments ± SEM. **P ≤ 0.001 determined by Student's t-test. **(H)** Immunoblots of HA-RTA^{E177Q} turnover in HEK293 cells treated with the indicated inhibitors for 4 hr and emetine for the indicated times.

Reporter	sgRNA	degradation rate (k)	r^2	normalized k	gene effect
GFP^{u*}	control	-0.034	0.998	1.000	0
	RNF139	-0.002	0.855	0.063	7.8
	UBE3C	-0.013	0.997	0.394	5.1
	UBE2D3	-0.023	0.985	0.681	4.4
	UBE2G2	-0.009	0.966	0.278	7.2
	UBE2J2	-0.019	0.997	0.558	3.6
	AUP1	-0.011	0.995	0.337	6.3
INSIG1-GFP	control	-0.027	0.960	1.000	0
	AMFR	-0.011	0.902	0.410	7.9
	UBE2G2	-0.005	0.999	0.179	7.7
	KCMF1	-0.021	0.970	0.772	2.6
	UBR4	-0.022	0.985	0.806	4.7
	UBE2D3	-0.018	0.998	0.672	5.4
$A1AT^{NHK}$-GFP	control	-0.009	0.999	1.000	0
	SYVN1	-0.002	0.984	0.250	6.1
	HERPUD2	-0.004	0.931	0.429	3.8
	UFM1	-0.006	0.984	0.668	4
	UBA5	-0.006	0.981	0.674	3.5
	UFC1	-0.007	0.992	0.707	3.3
	UFL1	-0.006	0.987	0.674	2.4
	DDRGK1	-0.007	0.984	0.734	3.4
	CDK5RAP3	-0.006	0.992	0.696	1.9
	UFSP1	-0.010	0.995	1.033	0.3
	UFSP2	-0.007	0.991	0.728	3.7
GFP-RTA^{E177Q}	Control	-0.080	0.959	1.000	0
	HERPUD2	-0.031	0.975	0.389	3.5
	UFM1	-0.048	0.949	0.597	4.9
	UBA5	-0.048	0.939	0.595	4.5
	UFC1	-0.049	0.949	0.618	4.5
	UFL1	-0.048	0.960	0.600	3.8
	DDRGK1	-0.053	0.989	0.664	3.5
	CDK5RAP3	-0.050	0.985	0.628	2.1
	UFSP1	-0.073	0.944	0.910	-0.5
	UFSP2	-0.051	0.954	0.644	3.8

Table S4. Related to Figure 1. Degradation rates and gene effects measured for the genes shown in Fig. 1E.